

Nitrogen Base Poisoning of NiMo Liquefaction Catalysts: A Kinetic Study

Bruce D. Adkins, Diane R. Milburn and Burtron H. Davis

Kentucky Energy Cabinet Laboratory
P. O. Box 13015, Iron Works Pike
Lexington, Kentucky 40512

INTRODUCTION

A mechanistic model has been proposed to explain coking on hydrotreating catalysts from four process configurations of the Wilsonville, AL coal liquefaction pilot plant (ref. 1). This model, which utilizes reversible adsorption of nitrogen bases on acid sites, and irreversible poisoning of these sites by sodium, can explain all of the trends seen in the elemental compositions of the catalysts used in six pilot plant runs spanning four process configurations, two coals and two catalysts. The model, presented here for Bronsted acid sites, is:



where CH represents an acid site capable of chemisorbing either one nitrogen base molecule or one sodium atom and BH represents another type of site capable of reacting with sodium but not the nitrogen base. NB_L represents a group of nitrogen bases associated with distillate solvent or light thermal resid (LTR) from the Critical Solvent Deashing unit (CSD) and having a lower average molecular weight than NB_H , which represents basic nitrogen compounds having a higher average molecular weight, associated with the thermal resid stream (TR) from the CSD. $\text{C}^-(\text{NB}_L\text{H})^+$ and $\text{C}^-(\text{NB}_H\text{H})^+$ are the acid-base adducts formed on the catalyst surface. ANa is the sodium present in coal ash, and CNa and BNa are the Na-exchanged acid sites. The essence of this mechanism is that NB_L , NB_H , and Na can exchange on the catalyst surface.

In considering the proposed exchanges, the question of overall rate control must be addressed. A simple kinetic analysis is presented in an attempt to determine whether adsorption, k_a , or desorption, k_d , is controlling these exchanges.

Kinetic Analysis

For an exchange between species "1" and "2", illustrated in reactions (1) and (2) or in (2) and (3):

$$\ln \frac{1 - k_1^* \theta_1}{1 - k_1^* \theta_1^*} = k_2^* t \quad (5)$$

where

$$k_1^* = \frac{k_{a1} + k_{d2}k_a^*}{k_a^* k_{d2}}$$

$$k_2^* = \frac{k_{d1} + k_{d2}k_a^*}{1 + k_a^*}$$

and

$$k_a^* = \frac{k_{a1}[1]}{k_{a2}[2]} = \text{"Adsorption selectivity"}$$

where k_a 's represent first-order adsorption rate constants, k_d 's represent first-order desorption rate constants, θ_1 is the fractional surface coverage of species "1" at any time, and θ_1^* is the initial surface coverage of "1". Pseudosaturation throughout the exchange is assumed in equation (5), such that $\theta_1 + \theta_2 = 1$.

Solving for the three specific reactions proposed in the model, we obtain for the exchange of NB_L-NB_H shown in reactions (1) and (2):

$$\ln(1 - k_{1,NB_H-NB_L}^* \theta_{NB_H}) = -k_{2,NB_H-NB_L}^* t \quad (6)$$

where:

$$\theta_1 = \theta_{NB_H}$$

$$\theta_{NB_H}^* = 0$$

$$k_{1,NB_H-NB_L}^* = \frac{k_{d,NB_H} + k_{a,NB_H-NB_L}^* k_{d,NB_L}}{k_{a,NB_H-NB_L}^* k_{d,NB_L}}$$

$$k_{2,NB_H-NB_L}^* = \frac{k_{d,NB_H} + k_{a,NB_H-NB_L}^*}{1 + k_{a,NB_H-NB_L}^*}$$

$$k_{a,NB_H-NB_L}^* = \frac{k_{a,NB_H}[NB_H]}{k_{a,NB_L}[NB_L]}$$

The exchange shown in equations (2) and (3), of NB_H and Na yields:

$$\ln = \frac{1 - k_{1,NB_H-Na}^* \theta_{NB_H}}{1 - k_{1,NB_H-Na}^*} \quad (7)$$

where:

$$\theta_1 = \theta_{NB_H}$$

$$\theta_{NB_H}^0 = 1$$

$$k_{1,NB_H-Na}^* = \frac{k_{d,NB_H} + k_{a,NB_H-Na}^* k_{d,Na}}{k_{a,NB_H-Na}^* k_{d,Na}}$$

$$k_{2,NB_H-Na}^* = \frac{k_{d,NB_H} + k_{a,NB_H-Na}^* k_{d,Na}}{1 + k_{a,NB_H-Na}^*}$$

$$k_{a,NB_H-Na}^* = \frac{k_{a,NB_H} [NB_H]}{k_{a,Na} [ANa]}$$

The form of equation (7) is troublesome if $k_{d,Na} \ll k_{d,NB_H}$. For irreversible sodium chemisorption, a better form is:

$$\ln \theta_{NB_H} = -k_{d,NB_H-Na}^* t \quad (8)$$

where:

$$k_{d,NB_H-Na}^* = \frac{k_{d,NB_H}}{1 + k_{a,NB_H-Na}^*}$$

I. Kinetics Calculated from Process Data

Carbon, nitrogen and sodium analyses were used to solve equations (6) through (8) for the various runs examined (ref. 1). Full coverage of NB_L is determined by the carbon content at saturation in the DITSL runs, which is reached very early in the run, and full coverage of NB_H is estimated by extrapolating the RITSL carbon data to 0% Na. θ_{NB_H} is then:

$$\theta_{NB_H} = \frac{C - C_{NB_L}}{C_{NB_H} - C_{NB_L}} \quad (9)$$

where C represents % carbon, C_{NB_L} is the % carbon present at saturation of NB_L , and C_{NB_H} is the % carbon present at full coverage of NB_H . An example of the fit for this exchange is shown in Figure 1a.

Nitrogen analyses are used in solving for the NB_H -Na exchange, making the analyses easier and more certain by eliminating the assumption that all carbon on the catalyst is present in the form of chemisorbed basic nitrogen. A sample of the fit of equation (8) to these data is shown in Figure 1b. Difficulties were encountered attempting to fit eqn. (7), which suggested the irreversible case (eqn. 8) be used instead.

The results obtained by fitting the model to the data allow examination of the two factors controlling the overall rate exchanges on the catalyst: rate(s) of nitrogen base desorption (k_d 's) and the adsorption selectivity for the two competing species (k_a^*). The relationships for limiting cases in the NB_L-NB_H exchange are shown in Table 1, and for the NB_H-Na exchange in Table 2.

II. Kinetics of Laboratory Desorption of Nitrogen Bases

Laboratory experiments were conducted using a CSTR to test the critical assumption that the nitrogen bases desorb from the catalyst. In two separate experiments blends of DITSL catalysts, still in the original process oil, were placed in the reactor extracted in flowing THF at 120°C, the gently stirred in tetralin feed at 250°C and 2000 psi for three weeks. Samples were taken, twice weekly, after cooling and depressurizing the reactor. Analyses of the catalyst showed a decrease in both nitrogen (from 0.45% to a fairly stable 0.15%) and carbon for the first two weeks, after which time a non-nitrogen containing coke formation was seen, probably tetralin derived carbon on the acid sites exposed by base desorption. A value of 0.04 day^{-1} was obtained for $k_{d,NB}$, which is in good agreement with the values from Tables 1 and 2, considering the effects of the non-nitrogen containing coke have been ignored. However, readsorption of nitrogen bases cannot be ruled out as the concentration of desorbed based present in the reactor could have been as high as 200 to 500 ppm at any time.

III. Comparison with Kinetics of Nitrogen Base Poisoning of Cracking Catalysts

Extensive literature exists on nitrogen base and alkali poisoning of cracking catalysts (e.g., ref. 2). Much less information is available on the poisoning of acidic hydrotreating catalysts, such as Shell 324. We can use cracking catalyst measurements in an attempt to rationalize the kinetic measurements obtained from process and laboratory data. However, the acidity of Shell 324 is likely to be different from that of silica-alumina cracking catalysts.

One of the earliest of these studies was performed by Mills, et al. (ref. 3) in which they studied the adsorption of quinoline on silica/alumina cracking catalysts at 315°C and several pressures. They identified two distinct kinetic regions in the desorption curve, corresponding to what they termed a rapidly desorbing "physisorbed" species, followed by a much slower "chemisorbed" species. Much later Kittrell, et al. (ref. 4) calculated rate constants from these data and suggested that the adsorption and desorption rates for the more rapidly desorbed quinoline should be used to predict reversible nitrogen poisoning of cracking catalysts. The numbers he obtained were approximately $k_a = 200 \text{ day}^{-1}$, $k_d = 150 \text{ day}^{-1}$. An attempt to obtain order-of-magnitude consistency between Kittrell et al.'s rate constants and our measurements yields the following relative rates:





Thus, if k_a and k_d of the NB_L group (which is estimated to have an overall stoichiometry very similar to that of quinoline) are as large as 200 day^{-1} and 150 day^{-1} respectively, a large kinetic difference in the NB_L and NB_H species is indicated. It would be highly speculative at this point to assume that these are the two species observed in reference 3. The main inconsistency with this picture is the rapid saturation of NB_L and NB_H on fresh sulfided catalyst beds that is clearly seen in DITSL and RITSL data.

Next let us assume that the nitrogen bases adsorb rapidly, but is very slow to desorb, analogous to the second species proposed by Mills et al., and using our CSTR measurement of $k_d = 0.05 \text{ day}^{-1}$. Fitting the calculations to our model for this case yields:



This ranking accommodates the rapid saturation of RITSL and DITSL with NB_H and NB_L .

IV. Gravimetric Vapor Phase Experiments

The questions raised in this kinetic study can only be answered by kinetic measurements using a differential flow reactor adsorption and desorption. Thus, a high pressure gravimetric reactor system, shown schematically in Figure 2, has been constructed. This will allow us to measure the adsorption and subsequent desorption of several nitrogen compounds at different pressures, and determine their kinetic rate constants. The ability to introduce hydrogen should also shed light on the HDN performance of this catalysts.

ACKNOWLEDGMENT

This work was supported by the Commonwealth of Kentucky, Kentucky Energy Cabinet and DOE Contract No. DE-FC-22-85PC80009 as part of the Consortium for Fossil Fuel Liquefaction Science (administered by the University of Kentucky).

REFERENCES

1. D. R. Milburn, B. D. Adkins and B. H. Davis, ACS Div. Fuel Preprints, **33** (2), 380 (1988).
2. T. F. Degnan and M. Farcasiu, U.S. Patent No. 4,550,090, October 29, 1985.
3. G. A. Mills, E. R. Boedeker and A. G. Oblad, J. Am. Chem. Soc., **72**, 1554, (1950).
4. J. R. Kittrell, P. S. Tam and J. W. Eldridge, Hyd. Proc., **63** (1985).

Table I.
Kinetic Analyses of NB_L - NB_H Exchanges

Limiting Case – Preferential Chemisorption		
NB_H (day ⁻¹) ($k_s^* NB_H NB_L \gg 1$)	$k_d, NB_L \approx 0.1$	$k_d, NB_L \approx 0.1$
NB_L (day ⁻¹) ($k_s^* NB_H NB_L \ll 1$)	$k_d, NB_L, k_s^* NB_H NB_L \approx 0.1$	$k_d, NB_L, k_s^* NB_H NB_L \approx 0.1$

Table II.

Kinetic Analyses of NB_H -Na Exchanges

	Wyodak-Shell 324M	Illinois #6-Shell 324M	Illinois #6-Amocat 1C (No Ash Recycle)	Illinois #6-Amocat 1C (Ash Recycle)
Limiting Case – Preferential Chemisorption				
NB_H (day ⁻¹) ($k_s^* Na NB_H \ll 1$)	$k_d, NB_H, k_s^* Na NB_H \approx 0.02$	$k_d, NB_H, k_s^* Na NB_H \approx 0.006$	$k_d, NB_H, k_s^* Na NB_H \approx 0.006$	$k_d, NB_H, k_s^* Na NB_H \approx 0.02$
Na (day ⁻¹) ($k_s^* Na NB_H \gg 1$)	$k_d, NB_H \approx 0.02$	$k_d, NB_H \approx 0.006$	$k_d, NB_H \approx 0.006$	$k_d, NB_H \approx 0.02$

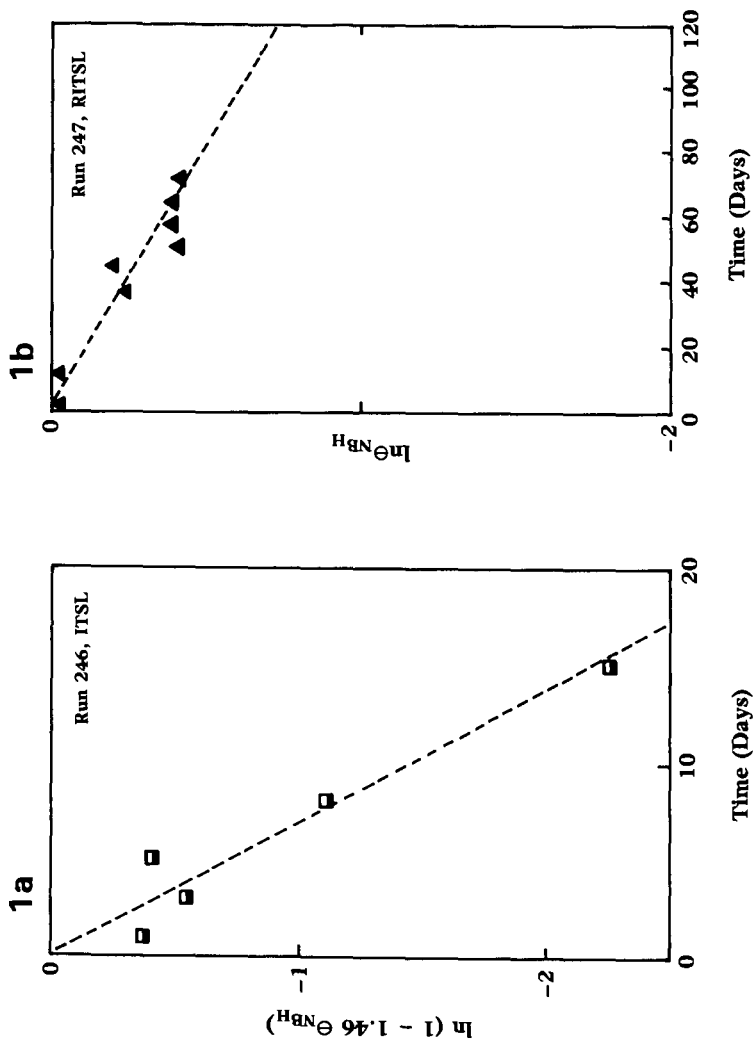


Figure 1a. Process data for the NB_L - NB_H exchange fitted to equation (6).
 Figure 1b. Data from the NB_L -Na exchange fitted to equation (8).

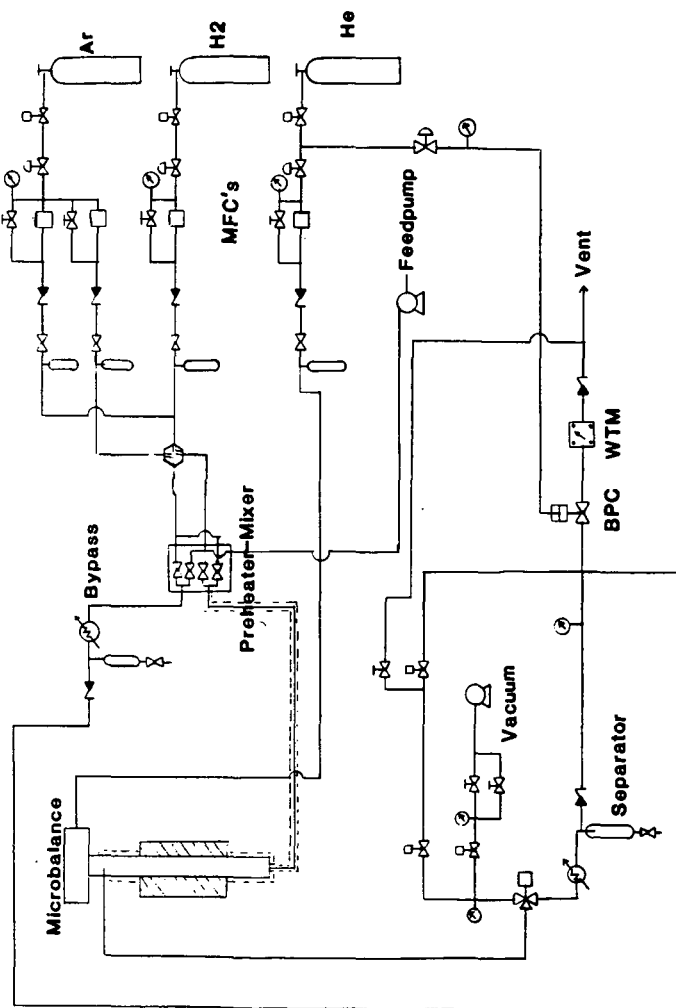


Figure 2. Schematic diagram of the high pressure gravimetric reactor system.